

EFFICIENT PHASE SPACE DENSITY CONSTRUCTION VIA TRANSFER OPERATORS*

V. B. Tembo[†], D. T. Abell, I. Haber, T. M. Antonsen
University of Maryland, College Park, MD, USA

Abstract

Finding invariant phase space level curves for large ensembles of particle trajectories is a core challenge for studying systems subject to complex Hamiltonian or weakly dissipative dynamics, such as beam and accelerator physics. These curves characterize long-term system behaviour and are critical for assessing stability, confinement, and matched beam transport. Direct methods rely on expensive particle pushing and tracking. We developed a fast, transfer-operator-based approach for finding invariant phase space surfaces that leverages sparse matrix computation to construct approximate invariant densities directly from trajectory data, enabling efficient level curve discovery while integrating with existing codes.

INTRODUCTION

We can understand the long-term behaviour of dynamical systems if we can characterize their invariant density distributions. Direct approaches involve pushing large ensembles of particles over long distances to accumulate sufficient information to approximate the invariant measure. While conceptually straightforward, this approach becomes computationally prohibitive for these systems. A way around this is to use transfer operators that encode the essential dynamical information without requiring exhaustive trajectory integration. The key is that the information needed to determine invariant densities lies in the local transition probabilities between different regions of phase space, rather than in the detailed long-term evolution of individual trajectories.

METHODOLOGY

The procedure we employ has two steps. First, data is collected describing in detail the trajectories in phase space over a finite distance or time. Typically, this data will come from a simulation code. However, in this paper, we use a map to generate the data. Then, instead of continuing the detailed simulation over longer periods of time to determine the asymptotic phase space density, a transfer operator is constructed based on the collected data that efficiently advances the phase space density directly. A similar method has been used to characterize magnetic flux surfaces in 3D plasma confinement configurations [1].

In the first step, phase space is discretized into an array of bins, with each bin labelled by an integer index i . For each particle in the data set, we record its starting and

ending bin number. Then a sparse transfer matrix F_{ij} is constructed by recording the fraction of trajectories that begin in bin i and terminate in bin j after one iteration. Trajectories that exit the phase space domain are discarded, and the corresponding matrix entries F_{ij} for out-of-bounds destinations are set to zero.

The invariant density distribution is obtained through iterative evolution of a density field using the constructed transfer matrix. At each iteration n , the density in bin j , d_n^j is updated according to:

$$d_{n+1}^j = \frac{1}{2} \left(d_n^j + \sum_i F_{ij} d_n^i \right). \quad (1)$$

This evolution equation is a weighted average between the previous density and the density predicted by the transfer matrix, with equal weighting factors of 1/2 chosen to provide numerical stability by damping high-frequency oscillations in the density field.

Following each matrix evolution step, numerical diffusion may be applied to account for the inherently dissipative nature of the physical system and to compensate for discretization effects. The diffusion scheme employs nearest-neighbour averaging, where each bin transfers a fraction of its density (determined by a diffusion strength parameter) to its four neighbouring bins. We note that the process of binning the density introduces a numerical diffusion, as there is often more than one receiving bin- j for a given sending bin- i . While the diffusion is artificial, it has been found in another application [2] to be advantageous. After diffusion, the density field is renormalized to maintain the constraint $\sum_j d_n^j = 1$.

RESULTS: APPLICATION TO THE STANDARD MAP

We take as our system the standard map. Trajectories in the (p, θ) plane are advanced according to:

$$\begin{aligned} p_{n+1} &= p_n + \Delta \sin \theta_n \\ \theta_{n+1} &= \theta_n + p_{n+1} \end{aligned}$$

Although the mapping is periodic in both variables, we take a trajectory for which p_n falls outside the interval $|p| < \pi$ to be out of bounds. The initial density is taken to be independent of θ and peaked at $p = 0$. The results of a sample calculation are shown in Fig. 1. Pictured in color is the converged density map on a square grid of 500x500 bins. Overlaying the density plot is a trajectory generated by iterating the standard map 250 times. On the right, is a line plot of the density as a function of p evaluated at $\theta = \pi$.

There are two issues of convergence that we have addressed. The first is the convergence of the density with

* This work supported in part by the US Department of Energy, Office of Science, Office of High Energy Physics, under Grant #DE-SC-0025277
† vtembo@umd.edu

iterations of the transfer matrix, Eq. (1). To monitor this, at each iteration we evaluate:

$$\text{NRMS}_{n+1} = \frac{\langle (d_i^{(n+1)} - d_i^{(n)})^2 \rangle}{\langle (d_i^{(n)})^2 \rangle},$$

where the angular brackets imply average over bins. The iteration process continues until the NRMS falls below a specified threshold, typically set to 0.001. Convergence is generally achieved within 20 to 30 iterations. The resulting converged density satisfies the physical constraints that all bins have non-negative density and densities go to zero at the leaky boundaries.

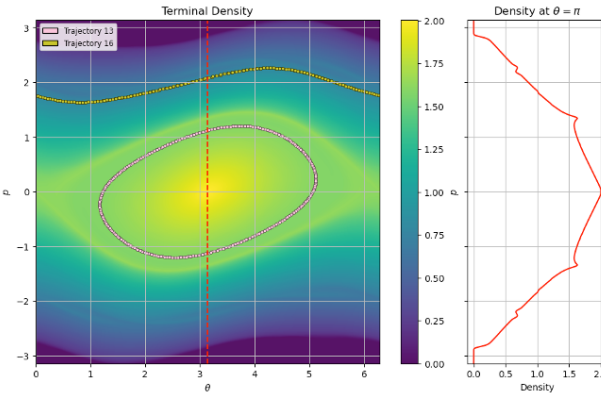


Figure 1: Trajectories overlaid on density map.

The accuracy of the converged invariant density is validated through direct comparison with individual map trajectories. Twenty validation trajectories, each consisting of 250 iterations, are selected from regions away from the leaky boundaries to ensure representative coverage of the phase space dynamics. These trajectories are overlaid on the converged density map, with interpolated density values assigned to each trajectory point from the surrounding grid cells. Figure 1 demonstrates this validation approach using two representative trajectories overlaid on the converged density contours. The trajectories exhibit clear alignment with the density structure, following the contour lines of the invariant measure.

Quantitatively, the accuracy of the method is assessed using the coefficient of variation (CV) of density values along the individual map trajectories. For each validation trajectory k , the coefficient of variation is computed as $\text{CV}_k = \sigma_k / \mu_k$, where σ_k and μ_k represent the standard deviation and mean of interpolated density values along trajectory k , respectively. The evolution of CV with iteration number provides a direct measure of convergence accuracy, as trajectories in a true invariant density should exhibit minimal variation in density values along their path. Sample results appear in Fig. 2 and Fig. 3

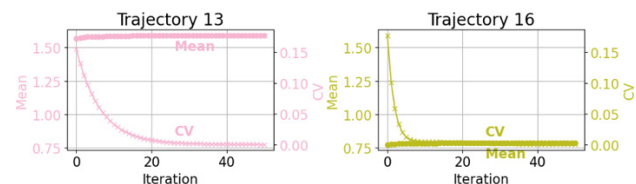


Figure 2: Mean and CV vs. iteration number.

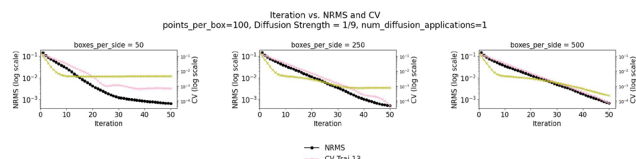


Figure 3: NRMS/CV vs. iteration number across scales.

The CV analysis demonstrates rapid convergence across multiple grid resolutions. For 50×50 , 250×250 , and 500×500 grid configurations, the coefficient of variation decreases sharply within the first 20 iterations and approaches a stable floor value determined by the discretization resolution. The convergence behaviour remains consistent across different grid sizes, with finer grids achieving lower asymptotic CV values due to reduced discretization error. This systematic reduction in CV with iteration number confirms that the sparse matrix approach successfully identifies invariant density structures with quantifiable accuracy that scales predictably with computational resolution.

CONCLUSION

This sparse transfer operator method is fast, accurate and compatible with existing codes such as WARP. We intend to use this tool when performing constrained optimizations on circular lattices. Here, we need to efficiently compute gradients of Figures of Merit with respect to lattice parameters while approximately maintaining moment periodicity of the beam. For this, the next step is to extend our method to particle pushes for trajectories subject to self-fields.

REFERENCES

- [1] M. Ruth and D. Bindel, “Level set learning for Poincaré plots of symplectic maps,” *SIAM J. Appl. Dyn. Syst.*, vol. 24, no. 1, pp. 611–632, Feb. 2025, doi:[10.1137/23m1622179](https://doi.org/10.1137/23m1622179)
- [2] P. Helander, S. R. Hudson, and E. J. Paul, “On heat conduction in an irregular magnetic field. Part 1,” *J. Plasma Phys.*, vol. 88, no. 1, Feb. 2022, doi:[10.1017/S002237782100129X](https://doi.org/10.1017/S002237782100129X)